

**CHITOSAN-COATED SILICA PARTICLES AS ANION TRAPPER
FOR ANTICORROSION COATING**



**A Report Submitted in Partial Fulfillment of the Requirements
for the Degree of Bachelor of Engineering (Petrochemical Engineering)
Department of Chemical Engineering, Faculty of Engineering,
King Mongkut's Institute of Technology Ladkrabang
Academic Year 2017**

This material is reserved for educational use only, not allowed for commercial use.

Forbidden to modify the content, and cite the document when use

การใช้อนุภาคซิลิกาที่หุ้มด้วยไคโตซานเพื่อดักจับประจุลบสำหรับชั้นเคลือบทนการกัดกร่อน



นางสาวศศิประภา รัตนานุกูล

ปริญญานิพนธ์นี้เป็นส่วนหนึ่งของการศึกษาตามหลักสูตร
วิศวกรรมศาสตรบัณฑิต สาขาวิชาวิศวกรรมปิโตรเคมี
ภาควิชาวิศวกรรมเคมี คณะวิศวกรรมศาสตร์
สถาบันเทคโนโลยีพระจอมเกล้าเจ้าคุณทหารลาดกระบัง
ปีการศึกษา 2560

This material is reserved for educational use only, not allowed for commercial use.

Forbidden to modify the content, and cite the document when use

Title Chitosan-Coated Silica Particles as Anion Trapper for Anticorrosion Coating

By Ms. Sasiprapa Rattananukul

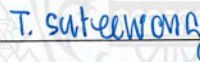
Field of Study Petrochemical Engineering

Advisor Asst. Prof. Dr. Teeraporn Suteewong
Asst. Prof. Ruenruedee Benjangkprasert

Accepted by the Faculty of Engineering, King Mongkut's Institute of Technology Ladkrabang in Partial Fulfillment of the Requirements for the Degree of Bachelor of Engineering (Petrochemical Engineering).

Thesis Committee

Chairman



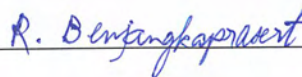
(Asst. Prof. Dr. Teeraporn Suteewong)

Committee



(Assoc. Prof. Dr. Duangkamol Na-Ranong)

Committee



(Asst. Prof. Ruenruedee Benjangkprasert)

Title Chitosan-Coated Silica Particles as Anion Trapper for Anticorrosion Coating

By Ms. Sasiprapa Rattananukul

Advisor Asst. Prof. Dr. Teeraporn Suteewong
Asst. Prof. Ruenruedee Benjangkaprasert

Field of Study Petrochemical Engineering

Affiliation Department of Chemical Engineering, King Mongkut's Institute of Technology Ladkrabang

Abstract

Coating is a simple but effective method in corrosion protection. Among the corrosive species, chloride ions are the important one, resulting in severe localized attack on metal substrate. Pitting corrosion then occurs. In this work, we develop anticorrosion coating, in which filler can absorb chloride ion. Chitosan-coated silica (SiO₂@CS) particles are synthesized and used as anion trapper. CS shell is crosslinked using tripolyphosphate (TPP). The synthesized particles are characterized by Fourier transform infrared spectroscopy (FTIR), Zeta-potential measurement and Transmission electron microscopy (TEM). FTIR and Zeta potential results indicate the presence of CS and TPP. Anticorrosion performance of composite coating on the stainless steel substrate tested using Potentiostat analysis. The results of the composite coating can use to increase corrosion resistance, decreasing corrosion rate.

Keywords: Chitosan, silica nanoparticle, tripolyphosphate and corrosion

เรื่อง	การใช้อนุภาคซิลิกาที่หุ้มด้วยไคโตซานเพื่อดักจับประจุลบสำหรับชั้นเคลือบทนการกัดกร่อน
โดย	นางสาวศศิประภา รัตนานุกูล
อาจารย์ที่ปรึกษา:	ผศ.ดร.ธีรพร สุธีวงศ์
อาจารย์ที่ปรึกษา	ผศ.รินฤดี เบญจางคประเสริฐ
สาขาวิชา	วิศวกรรมปิโตรเคมี
สังกัด	ภาควิศวกรรมเคมี สถาบันเทคโนโลยีพระจอมเกล้าเจ้าคุณทหารลาดกระบัง

บทคัดย่อ

การเคลือบผิวเป็นวิธีที่ง่ายและมีประสิทธิภาพในการใช้ป้องกันการกัดกร่อน ในบรรดาสารที่มีฤทธิ์กัดกร่อน ไอออนของคลอไรด์มีความสำคัญมากที่ทำให้เกิดการกัดกร่อนแบบรูเข็ม ซึ่งเป็นการกัดกร่อนที่รุนแรงและเกิดขึ้นที่ผิวของโลหะ ในงานวิจัยนี้เราได้พัฒนาสารเคลือบผิวเพื่อป้องกันการกัดกร่อนที่ประกอบด้วยอนุภาคที่สามารถดูดซับไอออนของคลอไรด์ได้ โดยอนุภาคดังกล่าวเตรียมจากอนุภาคซิลิกาที่เคลือบด้วยไคโตซาน ($\text{SiO}_2@CS$) แล้วทำการเชื่อมโยงโมเลกุลของไคโตซานที่ผิวด้วยไตรโพลีฟอสเฟต (TPP) จากการศึกษาโครงสร้างสัณฐานและการกระจายตัวของอนุภาคซิลิกาด้วยกล้องจุลทรรศน์อิเล็กตรอน (Transmission Electron Microscopy: TEM) พบว่าอนุภาคมีขนาด 237 ± 34 นาโนเมตร หมู่ NH_3^+ จากผล FTIR และศักย์เซต้าที่เป็นบวก บ่งชี้ว่ามีไคโตซานหุ้มบนผิวอนุภาค โดยศักย์จะมีความเป็นลบมากขึ้นหลังการเชื่อมโยงโมเลกุลไคโตซานด้วย TPP และสมบัติการกัดกร่อนของสารเคลือบผิวบนแผ่นสแตนเลสจะทำการทดสอบในสารละลาย NaCl (1%w/v) โดยใช้การวิเคราะห์ Potentiostat จากการตรวจวัดการกัดกร่อนพบว่า ชั้นเคลือบที่ประกอบด้วยอนุภาคที่สังเคราะห์ได้มีประสิทธิภาพในการลดอัตราการกัดกร่อน

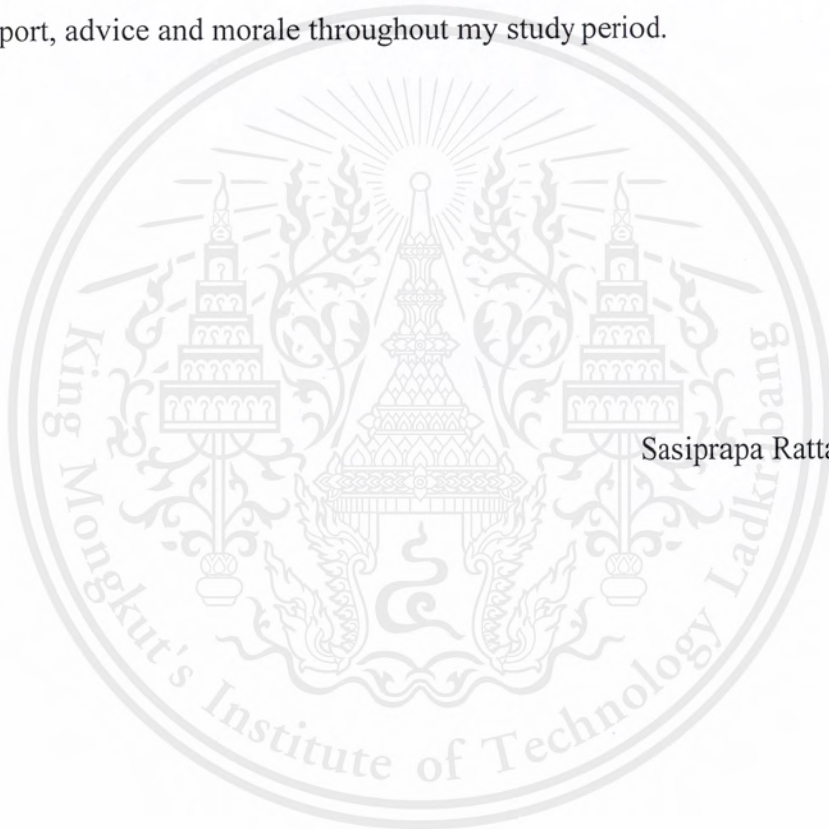
คำสำคัญ: ไคโตซาน การกัดกร่อนและอนุภาคซิลิกา

Acknowledgements

I am grateful to my thesis advisor, Asst. Prof. Dr. Teeraporn Suteewong and Asst. Prof. Ruenruedee Benjangkprasert for her invaluable help. Without her exemplary guidance and encouragement, this study would hardly have been completed.

In addition, I am grateful Mr. Paiboon Saejear for all suggestions and his help in this research.

Finally, I most gratefully acknowledge my parents and my friends for all their support, advice and morale throughout my study period.



Sasiprapa Rattananukul

CONTENTS

	Page
Abstract	I
Acknowledgements	III
Contents	IV
List of figures	VII
List of tables	IX
Chapter I Introduction	1
1.1 Background	1
1.2 Objectives	2
1.3 Scopes of Work	2
1.4 Expected Outputs	3
Chapter II Theory and Literature reviews	4
2.1 AISI Type 316L Stainless Steel	4
2.2 Corrosion	5
2.2.1 Corrosion reactions	5
2.2.2 Pitting corrosion	5
2.2.3 Mechanism of pitting corrosion	6
2.2.4 Autocatalytic nature of pitting corrosion	6
2.3 Corrosion protection coating	7
2.3.1 Corrosion protection and control using nanomaterials	7
2.3.2 Filler	8
2.4 Literature reviews	9

CONTENTS (Cont.)

	Page
Chapter III Research methodology	11
3.1 Chemicals and Materials	11
3.2 Equipment and Apparatus	12
3.3 Procedures	12
3.3.1 Synthesis of silica nanoparticles	12
3.3.2 Preparation of the tripolyphosphate – crosslinked chitosan and SiO ₂ nanoparticles	13
3.3.3 Preparation of steel plate	14
3.3.4 Preparation of composite coating on steel plate	14
3.4 Characterization	14
3.5 Corrosion performance tests	14
Chapter IV Results and Discussion	15
4.1 Morphology of silica nanoparticles	15
4.2 Surface Modification of tripolyphosphate (TPP) – crosslinked chitosan (CS) coated on SiO ₂ nanoparticles	16
4.3 Surface morphology of coating	18
4.4 Corrosion test	21
Chapter V Conclusion	25
References	26
Appendix	
28 Appendix A: Experimental data	29

CONTENTS (Cont.)

	Page
Appendix B: Results data	30
Appendix C: Calculation data	34



LIST OF FIGURES

	Page
Figure 2.1 Electrochemical reaction occurring during corrosion	5
Figure 2.2 Autocatalytic process reaction occurring in corrosion pit	7
Figure 3.1 Experiment set for synthesis of silica nanoparticles	13
Figure 4.1 TEM images of SiO ₂ nanoparticles	15
Figure 4.2 FTIR spectra of bare SiO ₂ nanoparticles, SiO ₂ @CS and SiO ₂ @CS/TPP.	16
Figure 4.3 Zeta potential values of bare and SiO ₂ @CS nanoparticles at various amount of chitosan	17
Figure 4.4 Zeta potential values of SiO ₂ @CS/TPP nanoparticles at various concentration of TPP (wt%).	17
Figure 4.5 SEM image of surface morphology of bare 316L stainless steel (A) magnification 500x, scale bar 10 μm; (B) magnification 3000x, scale bar 2 μm.	18
Figure 4.6 SEM image of GPTMS coating or pure epoxy (A) magnification 500x, scale bar 10 μm; (B) magnification 3000x, scale bar 2 μm.	19
Figure 4.7 SEM image of GPTMS/SiO ₂ coating (A) magnification 500x, scale bar 100 μm; (B) magnification 3000x, scale bar 2 μm.	19
Figure 4.8 SEM image of GPTMS/SiO ₂ /CS coating (A) magnification 500x, scale bar 100 μm; (B) magnification 3000x, scale bar 2 μm.	20

LIST OF FIGURES (Cont.)

	Page
Figure 4.9 SEM image of GPTMS/SiO ₂ /CS/TPP coating (A) magnification 100x, scale bar 100 μm; (B) magnification 500x, scale bar 2 μm.	20
Figure 4.10 Potentiodynamic polarization curves of various coating obtained at potential scan rate of 0.1 mV s ⁻¹ in 1% NaCl solution at 25°C. Using molecular weight of is 25 kDa. A, B, and C denoted concentration of TPP 0, 5, and 10 wt%, respectively.	21
Figure 4.11 Potentiodynamic polarization curves of various coating obtained at potential scan rate of 0.1 mV s ⁻¹ in 1% NaCl solution at 25°C. Using molecular weight of CS is 890 kDa. G, H, and I denoted concentration of TPP 0, 5, and 10 wt%, respectively.	22
Figure 4.12 Pitting potential value of (a); bare SS (b); GPTMS coating (c); GPTMS/SiO ₂ coating (d-e); GPTMS/SiO ₂ /CS coating (f-g); GPTMS/SiO ₂ /CS/TPP (5 wt%) coating	23
Figure 4.13 Pitting current density value of (a); bare SS (b); GPTMS coating (c); GPTMS/SiO ₂ coating (d-e); GPTMS/SiO ₂ /CS (25 kDa) coating (f-g); GPTMS/SiO ₂ /CS (890 kDa)/TPP coating	24
Figure B.6 FTIR spectra of SiO ₂ @CS at various CS concentration (25 KDa)	32
Figure B.7 FTIR spectra of SiO ₂ @CS at various CS concentration (890 KDa)	32

LIST OF TABLES

	Page
Table 2.1 Chemical composition and properties of AISI Type 316L stainless steel	4
Table 2.2 Nanocoatings in corrosion prevention	7
Table A.1 Chemical composition ratio in silica nanoparticles synthesis	29
Table A.2 List of analytical measurement that use study characterization	29
Table B.1 Zeta potential value of SiO ₂ nanoparticles	30
Table B.2 Zeta potential values of SiO ₂ @CS particles varying amount of CS	30
Table B.3 Zeta potential values of SiO ₂ @CS/TPP particles varying concentration of TPP	31
Table B.4 Pitting potential and pitting current density of bare SS and various coating	31
Table B.5 Efficiency of pitting corrosion protection (%) of bare SS and various coating	32

CHAPTER I

INTRODUCTION

1.1 Background

Corrosion is a major industrial problem. It is defined as the destruction of metal caused by the reaction between metal and corrosive species, leading to damage in the production process and economy. Stainless steel is widely used in the industry, for example, as beams for the structural framework in houses or plants, pipeline, cargo ship and drilling rig in seawater. When it is exposed to high amount of corrosive species, esp. sulfate and chloride ions, pitting corrosion occurs. Pitting corrosion is a type of corrosion caused by localized attack of aggressive anion, resulting in holes, which rapidly grow and damage metal ¹. Therefore, the efforts to develop more efficient methods to prevent corrosion have been ongoing and important.

Coating is a simple but effective method in corrosion protection. This method provides an additional physical barrier that delays the contact between metal and corrosive species. Its protecting efficiency can be enhanced by self-healing, corrosion inhibitor, reinforcing filler and ion trapper ². Most metals require the application of a protective coating especially, if there is a high risk for pitting corrosion. Anions such as chloride, bromide, sulfate, nitrate and carbonate are common corrosive species. Extending diffusion path length of these ions by adding particle filler in the coating matrix can be delayed corrosion process. If the filler in the coating absorb anions, the corrosion would be further slowdown. It thus leads to the concept of anion trapper. Kartsonakis et al. studied the anticorrosion performance of the coating on the alloy AA2024-T3. They incorporated diethylenetriamine modified SiO₂ particles. As a result, the protonation of these primary amine groups in diethylenetriamine became chloride trapper and increased the corrosion resistance of the coating ³. Zhou et al. studied the coating containing positively charged layered double hydroxides (LDHs) and negatively charged corrosion inhibitor. In this system, chloride ions were exchanged with anion inhibitor and were electrostatically trapped by cationic LDHs. So, corrosion protections were caused by corrosion inhibitor and anion trapper ⁴. Qian et al. reported anticorrosion coating prepared via polyelectrolyte-coated SiO₂. Chitosan (CS) was used

This material is reserved for educational use only, not allowed for commercial use.

natural cationic polyelectrolyte and polyaspartic was used anionic polyelectrolyte and corrosion inhibitor. The results showed excellent anticorrosion performance in the coating⁵. CS is a cationic biopolymer, containing primary amine group in the structure⁶. However, the CS as anion trapper has not yet been reported. Thus, would like to develop the anion trapper by combining advantages of CS and SiO₂ particles.

In this work, CS-SiO₂ particles are synthesized as anion trapper. CS is conjugated on the SiO₂ surface. Tripolyphosphate, corrosion inhibitor, is used to crosslink CS shell as well as exchanged with diffusing corrosives. Chloride ion from sodium chloride is used as anion representative. Effect of CS content and crosslink density on entrapment efficiency will be studied. Selected nanocomposite will be incorporated in epoxy coating for carbon steel and corrosion resistance will be discussed.

1.2 Objective

- 1.2.1 To develop anion trapper from CS-coated SiO₂ particles as anticorrosion filler

1.3 Scopes of Work

- 1.3.1 Synthesize silica nanoparticles and modify their surface with chitosan and tripolyphosphate.
- 1.3.2 Study the effect of CS content crosslink density on chloride trapping efficiency.
- 1.3.3 Study the corrosion resistance of epoxy coating containing the composite selected from 1.3.2

1.4 Expect outputs

- 1.4.1 Optimized protocol for the synthesis of CS-coated SiO₂ particles as anion trapper
- 1.4.2 Active multifunctional anticorrosion filler from CS-coated on SiO₂ particles as anion trapper



CHAPTER II

THEORY AND LITERATURE REVIEWS

2.1 AISI Type 316L Stainless Steel

AISI Type 316L stainless steel is an alloy, containing iron as the main component. The other metals are added to improve properties such as nickel to increase the tensile strength, chromium and molybdenum to increase corrosion resistance⁷. The composition of the 316L is shown in Table 2.1.

Table 2.1: Chemical composition and properties of AISI Type 316L stainless steel⁷

Component	wt%
Iron	Balance
Chromium	16.0 min. – 18.0 max.
Nickel	10.0 min. – 14.0 max.
Molybdenum	2.00 min. – 3.00 max.
Manganese	2.00
Carbon	0.03
Phosphorus	0.03
Sulphur	0.045
Silica	0.75

The stainless steel has been used in building as the beams for the structural framework in houses or plants, pipelines and bridges. It will be destroyed by environments such as air, moisture, chlorine, ammonia, hydrogen and sulfide⁸. When the metal is exposed to high amount of corrosive species, the corrosion occurs.

2.2 Corrosion

Corrosion is the destruction of a material because of reaction with the environment. It occurs on the same metal when atoms of the metal are oxidized and damaged the entire surface. The metal loses electrons to oxygen in the air or in water. As the oxygen is reduced, it forms an oxide with the metal as passive corrosion protection⁹.

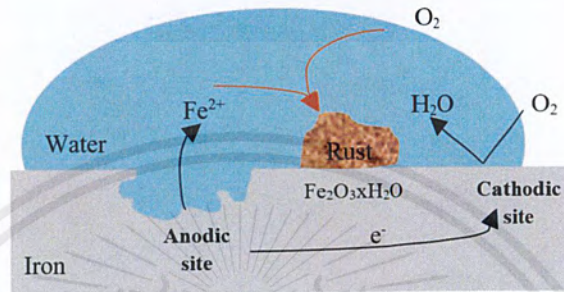
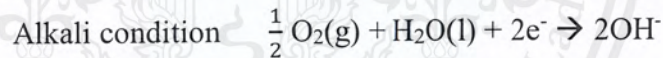


Figure 2.1 Electrochemical reaction occurring during corrosion

2.2.1 Corrosion reactions



The condition of a large amount of aggressive ion particularly chloride ion, bromide ion and iodine ion will be effective for the pitting corrosion

2.2.2 Pitting corrosion

Pitting is one of eight forms of corrosion, which is one of the most extreme localized attacking that cause the holes in the metal. Although, the holes can be visible in some small point, it is highly severe for metal¹. When the passive state of metal was attacked by exposing with chlorides, the corrosion risk is determined by the chloride content.

2.2.3 Mechanism of pitting corrosion

The pitting mechanism can be divided into 3 steps ¹⁰

1. *Adsorption*: Generally, the anion will move into the surface of the metal. The passive film will adsorb the anion and protect the reduction of the metal surface.
2. *Penetration*: The oxygen in the passive film will be replaced by anion resulted in the weak bond between oxide and metal. Thus, the anion can be moved into the surface metal.
3. *Film Breaking*: The anions caused by more electron losing until the metal cannot produce the passive film. Then, the breaking of film leads to enlargement of pitting corrosion

2.2.4 Autocatalytic nature of pitting corrosion

Pitting corrosion is an anodic reaction, an autocatalytic process that is the continuing activity of the pitting corrosion process by schematically illustrated in Fig 2 for a metal in an oxygenated NaCl solution. The pit is anodic and the metal surface is cathodic. The positive charge of metal attracts the negative charge from chlorine ion. The high concentration of metal and chloride is ready to react with water as a hydrochloric in the pit. It was found that the metal hydroxide and H^+ ions are accelerating the corrosion. In addition, the oxygen concentration in the pit is zero so it becomes the cathodic oxygen and reactions instead on the metal surface ¹.

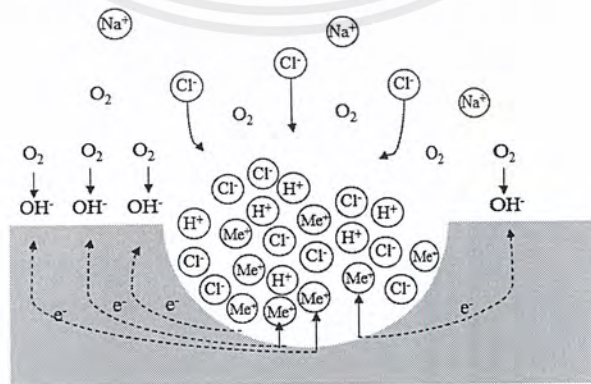


Figure 2.2 Autocatalytic process reaction occurring in corrosion pit

2.3 Corrosion protection coating

Coating for corrosion resistance can be provided one or more of the characters to protect the substrate of a metal. For example, an impermeable barrier to moisture and corrosive species, corrosion inhibitor and cathodic protection. The coating can be produced in single or more complex multilayer coating ².

2.3.1 Corrosion protection and control using nanomaterials

Nowadays, nanomaterials are interesting because of their performance in various fields. A nanocoating can be defined as the thickness of the coating in nanoscale and included the second phase that are nanoparticles. The nanoparticles are dispersed into the matrix of coating phase ¹¹.

Table 2.2 Nanocoatings in corrosion prevention¹¹

Thin films	Nanograined coatings	Nanocomposite coatings	Smart coatings
Ceramic, metallic, composite (nano/micro-grained), self-assembled monolayer	Ceramic, metallic, composite (thin/thick films)	Polymer-ceramic, metallic-ceramic, polymer-metallic	Replacement for conversion coatings, smart polymer coatings

The researches have been done on nanocomposite coating for various applications including corrosion prevention. Xianming Shi et al. studied the effect of nanoparticles, SiO₂, Zn, Fe₂O₃ and halloysite clay. These nanoparticles were dispersed in coated epoxy on the steel substrate. Then, they investigated the ability for anticorrosion and mechanical properties. The studied nanoparticles, Fe₂O₃ and halloysite clay were the best nanoparticles for corrosion resistant. Moreover, SiO₂ nanoparticles can be improve the microstructure and enhance the corrosion resistance and Young's modulus of the epoxy coating ¹². In recent years, the researcher has been studied the nanocomposite from natural materials. Suwadee et al. studied self-healing hybrid nanocomposite preparing the epoxy resin which contains self-healing agent (Perfluorooctyl triethoxysilane) loaded silica microcapsule. The results revealed the

This material is reserved for educational use only, not allowed for commercial use.

modified silica and self-healing microcapsule effectively increased the corrosion resistance and decreased the oxygen permeability in the coating ¹³. Kartsonakis et al. studied crosslinking between epoxy (bisphenol A diglycidyl ether) and modified silica that contained cerium molybdate as corrosion inhibitor. It was coated on magnesium alloy ZK10. The increased corrosion resistance results were revealed when tested in corrosive environment ¹⁴. Moreover, this coating was delaminated because the defect from gas and water occurs in process. The water was evaporated during drying of coating process results in holes in metal leads to localized corrosion occurs. Therefore, improving this problem is the addition of filler into the coating.

2.3.2 Filler

Filler is the material added to the resin in a small quantity to adjust the mechanical properties of coating. Normally, this additive is distributed into the matrix, there is no significant change in the structure of the matrix polymer. In general, additives should have the following properties ¹⁵:

1. Effective work
2. Stable under the conditions of usability
3. No bleeding and blooming
4. Non-toxic, have no taste and odor

There are many reports of improving the anticorrosion coatings by using nanoparticles such as; TiO_2 , ZnO , SiO_2 and organoclay.

2.4 Literature reviews

There are report about corrosive protection coating that focused on anion trapper, it can be divided into 2 features including organoclay from layered double hydroxide and modified surface silica with amine groups. Tedim et al. ¹⁶ studied Zn-Al layered double hydroxides (LDHs) as chloride nanotraps, which intercalated with nitrate anions. The working system will be respond with chloride concentration, then release the nitrates that interpolated in the middle of LDHs, ion-exchange equilibrium occurs. The ion-exchange is an exchange between nitrate ion and chloride ion in the coating. As a result, it can be delayed diffusion of anion to the metal. Thus, it proved that Zn-Al-LDHs is one of filler to protect corrosive species but there is some disadvantage of LDHs, it is an agglomeration of LDHs. However, researchers are interested in LDHs, resulting in the development of LDHs to improve these problem..

The another feature is modified surface silica with amine groups. Kartsonakis et al. ³ studied multifunctional epoxy containing a mixture of chloride trapper. The chloride trapper made from reaction between the epoxy group (3-glycidoxypropyltrimethoxysilane) and primary amine groups of diethylenetriamine structure. The resulting in the protonated of these amine groups as the chloride trapper. According to the principle in electrostatically between positively charged and negatively charged. Ramezanzadeh et al. ¹⁷ interested in amine group ability from organic materials. The graphene oxide as a filler in the coating. Graphene oxide was functionalized with p-phenylenediamine to be an amino-functionalized graphene oxide (FGO), then dispersed in an epoxy coating, coated on metal substrate. The results show that it is the good anticorrosion coating due to the covalent bonds of carboxylic and epoxide groups in FGO with amine groups in diamine. In addition, it affects to enhance the barrier and anticorrosion performance. The FGO increased the ionic resistance from the hydroxyl ions. Therefore, it can be prevented the diffusion of chloride ion from corrosive environment. It was found that the ability of amine group in organic materials are interesting to use as an anticorrosion coating.

Luckachan et al ¹⁸ studied organic polymeric material for anticorrosion coating. The coating was prepared by layer by layer of chitosan and polyvinyl butyral (PVB) on carbon steel substrate. In chitodan layer, silica was modified with glutaraldehyde as a self-healing agent, then it was dispersed in chitosan layer. The resulting, the chitosan

This material is reserved for educational use only, not allowed for commercial use.

Forbidden to modify the content, and cite the document when use

coating enhanced corrosion resistance due to conducting properties like a graphene reinforcement. In addition, anticorrosion of chitosan coating were tested in sodium chloride media, it can be anticorrosion resistance in a few days. Thus, the chitosan coating is the temporary for anticorrosion. Then, Qian et al.⁵ studied the chitosan performance to be anticorrosion coating. Silica nanoparticles were coated layer by layer electrostatic adsorption between positively charged and negatively charged of chitosan and polyaspartic respectively. Polyaspartic is a corrosion inhibitor. The results showed excellent performance of coating.

Positively charged of chitosan can be adjusted in our work to develop the efficient anion trapper for anticorrosion. The previously studied about modified of chitosan, which using glutaraldehyde as chemical crosslinking agent but it is toxic in their unreacted forms. To improve this problem, natural crosslinking agent, tripolyphosphate is selected due to it has low molecular weight anions. In addition, the tripolyphosphate performance acts as corrosion inhibitor. The studied of Fahim et al.¹⁹ used sodium tripolyphosphate (STPP) as corrosion inhibitor of mild steel. They revealed that when increasing the concentration of sodium tripolyphosphate (STPP), increasing inhibition efficiency.

CHAPTER III

RESEARCH METHODOLOGY

This work focuses on the development of anticorrosion coating containing anion trapper using chitosan-coated SiO₂ nanoparticles (SiO₂@CS). SiO₂ nanoparticles are first synthesized via Stöber-based sol-gel method using tetraethyl orthosilicate (TEOS) as a silica precursor. Then, the surface of silica nanoparticles is coated with CS. CS layer is crosslinked with tripolyphosphate (TPP) in acidic condition. Resulting composites are dispersed in epoxy matrix and corrosion investigated by using 1% NaCl solution as a test media. Surface morphology and thickness of coating is studied by Scanning Electron Microscopy (SEM).

3.1 Chemicals and Materials

1. Tetraethyl orthosilicate (GC grade)
2. Ammonia solution (Analytical reagent grade)
3. Methanol (Commercial grade)
4. Ethanol (Commercial grade)
5. Chitosan (MW= 25 and 890 kDa, Food grade)
6. Sodium tripolyphosphate (Commercial grade)
7. Acetic acid (Analytical reagent grade)
8. 3-Glycidoxypropyltrimethoxysilane (KBM-403)
9. Sodium chloride (Food grade)
10. Sodium hydroxide
11. Deionized water
12. Sulfuric acid
13. Stainless steel (AISI 316L)

3.2 Equipment and Apparatus

1. Erlenmeyer flask
2. Round bottom flask
3. Beaker
4. Pipette and micropipettes
5. Temperature-controlled magnetic stirrer
6. Magnetic bar
7. Centrifuge
8. Centrifuge tubes
9. Stands and clamps
10. Spatulas
11. Stirring rod
12. Parafilm
13. Oven

3.3 Procedures

3.3.1 Synthesis of silica nanoparticles²⁰

- 1) Add MeOH (300 ml) in round bottom flask (500 ml). Stir the solution at 340 rpm. Then, add DI water (30 ml) and NH_4OH (37.5 ml).
- 2) While stirring, add TEOS, 15 ml into the mixture in 1) and stir for 120 minutes. The color of the reaction mixture changed from colorless to turbid as shown in Figure 3.1



Figure 3.1 Experiment set for synthesis of silica nanoparticles

- 3) To remove the unreacting chemicals, the solution was centrifuged at 8,000 rpm for 7 minutes. Remove supernatant and redisperse the particles in ethanol. Repeat the centrifugation 3 times
- 4) Store cleaned silica nanoparticles in ethanol

3.3.2 Preparation of the tripolyphosphate – crosslinked chitosan and SiO₂ nanoparticles ²¹

- 1) Prepare the chitosan solution by dissolving 2 g. of chitosan in 100 ml of dilute acetic acid (2% v/v)
- 2) Add 1.2 g of SiO₂ nanoparticles in the mixture of chitosan, then sonicate and stir for 15 min.
- 3) Add the mixture in previous into 100 ml of 5,10 w% sodium tripolyphosphate solution (pH=3)
- 4) Stir the mixture in 3) for 18 hrs.
- 5) Wash with deionized water and separate by centrifugation
- 6) Repeat the depositing, where the resulting system has a final centrifuge 5 times or pH constant at 5

3.3.3 Preparation of steel plate

- 1) Prepare a AISI stainless steel 30 X 30 mm
- 2) Wash the steel plate using deionized water
- 3) Scrub with abrasive paper 100 and 1000 grit for 6 min

3.3.4 Preparation of composite coating on steel plate

- 1) Mix 1 ml of methanol and 1 ml of GPTMS into the container
- 2) Add 0.018 g of nanocomposites and stir for 5 min
- 3) Attach the steel plate on a spin coater and set the spin rate at 250 rpm
- 4) Drop 2 ml of the solution on a steel plate and wait for 5 min
- 5) Adjust the spin rate to 500 rpm. And wait for 1 min
- 6) Dry the sample in the oven at 120 °C for 12 hrs

3.4 Characterization

- 1) Particle size distribution and morphology of silica nanoparticles is characterized by Transmission electron microscopy (TEM, FEI TECNAI T20 G2).
- 2) Surface functionalization of silica nanoparticles before and after modified is studied using Fourier transform infrared spectroscopy (FTIR, Perkin Elmer, Spectra GX).
- 3) Zeta potential of synthesized particle is measured by Zetasizer Nano ZS (Malvern measurement)
- 4) Surface morphology and thickness of coating layer is investigated by Scanning electron microscope (SEM, EVO MA 10 Versatile multipurpose SEM).

3.5 Corrosion performance tests

- 1) Corrosion performance of coating in 1% NaCl is tested by Potentiostat techniques (Autolab PGSTAT302N)

CHAPTER IV

RESULTS AND DISCUSSION

This project aims to improve anticorrosion properties of epoxy coating by incorporating SiO₂@CS in the coating layer. SiO₂ was first synthesized via Stöber method. CS is then coated on the surface of silica nanoparticles (SiO₂) and crosslinked with tripolyphosphate (TPP).

4.1 Morphology of silica nanoparticles

Figure 4.1 shows TEM images of non-modified SiO₂ nanoparticles. Based on particle size analysis using ImageJ, the particles are about 235±34 nm and monodispersed.

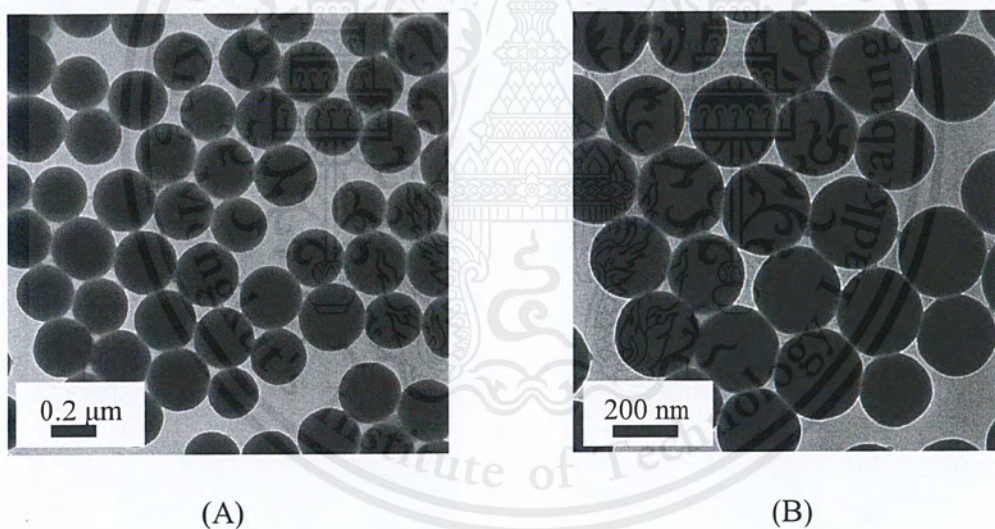


Figure 4.1 TEM images of SiO₂ nanoparticles (A) magnification 9600x, scale bar 0.2 μm; (B) magnification 14500x, scale bar 200 nm.

4.2 Surface Modification of tripolyphosphate (TPP) – crosslinked chitosan (CS) coated on SiO₂ nanoparticles (SiO₂@CS/TPP)

SiO₂ nanoparticles were modified with 2 different molecular weight of chitosan (25 and 890 kDa) followed by crosslinking with tripolyphosphate. SiO₂@CS and SiO₂@CS/TPP are denoted as CS-coated silica and TPP-crosslinked CS coated SiO₂, respectively. The presence of CS and TPP were characterized using FTIR and Zetasizer analysis.

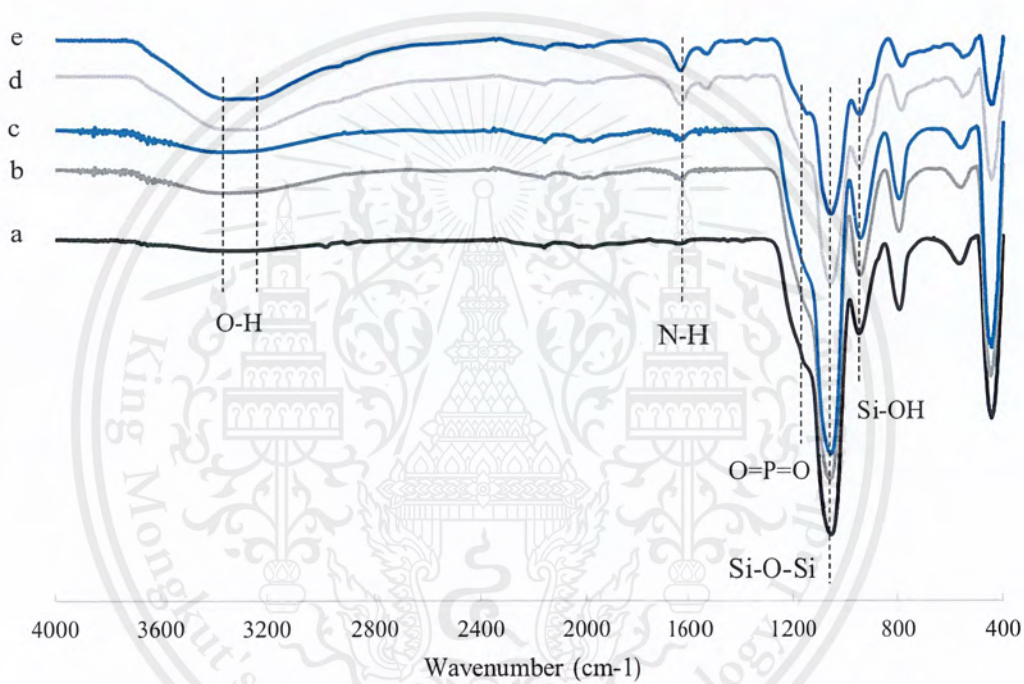


Figure 4.2 FTIR spectra of (a) bare SiO₂ nanoparticles and (b,c) SiO₂@CS (25 and 890 kDa, respectively); (d,e) SiO₂@CS (25 and 890 kDa, respectively)/TPP.

All FTIR spectra displayed in Figure 4.2 show the characteristic peaks of silica at 1052 and 940-950 cm⁻¹, corresponding to Si-O-Si and Si-OH group, respectively. All coated samples (b-e) exhibit peaks at 1628 cm⁻¹, corresponding to N-H group of chitosan. The additional peak at 1183 cm⁻¹ of PO₂ can be observed in sample d and e, confirming the presence of tripolyphosphate ions. From FTIR spectra, it can be confirmed the conjugation of TPP-crosslinked chitosan on the silica surface.

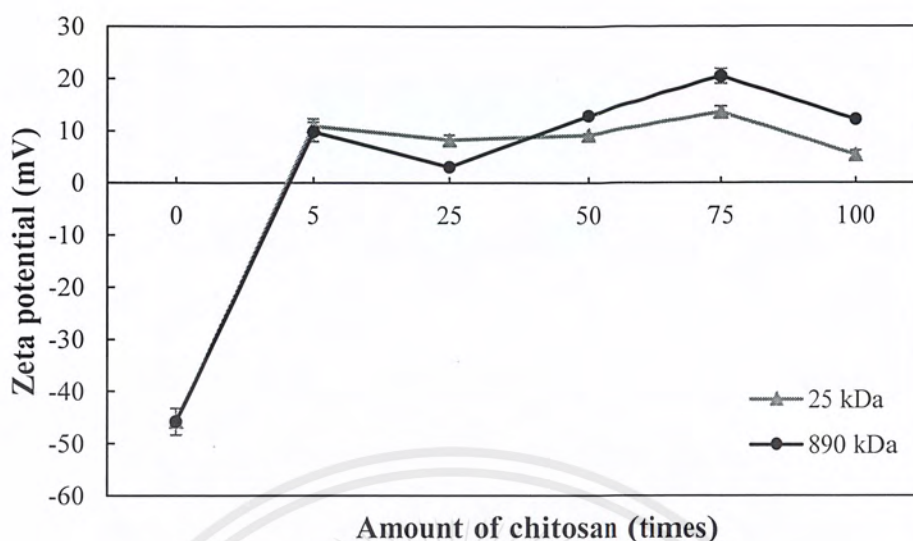


Figure 4.3 Zeta potential values of bare and SiO₂@CS nanoparticles at various amount of chitosan, (MW of CS used are 25 and 890 kDa).

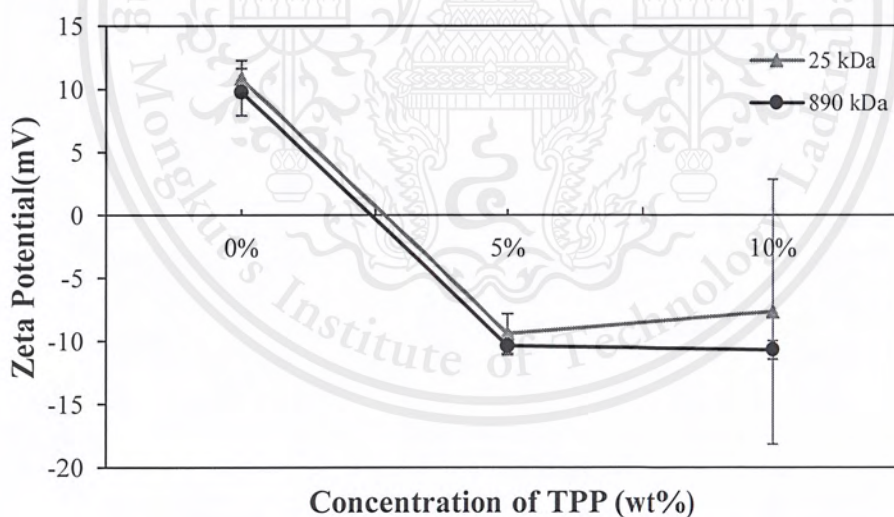


Figure 4.4 Zeta potential values of SiO₂@CS/TPP nanoparticles at various concentration of TPP (wt%).

Zeta potential values of SiO₂@CS are shown in Figure 4.3 After coating with CS, zeta potential of SiO₂ increases from negative potential (-45.80 mV) to +05 - +20 mV, indicating the presence of cationic polysaccharide of chitosan on of SiO₂²². This material is reserved for educational use only, not allowed for commercial use.

In addition, the amount of CS is varied in this experiment (0, 5, 25, 50, 75 and 100 times from initial ratio, 2 g. CS of 1.2 g. SiO₂) in order to study the presence of CS on the SiO₂ surface. The increase in CS concentration from 5-75 times in coating enhanced the zeta potential of SiO₂@CS. At 100 times CS, zeta potential became lower because of the electrostatic charge repulsion between the chains. However zeta potential values of all SiO₂@CS suggests that they are not colloidal stable, in terms of electrostatic stabilization, since they are lower than +30 mV²³.

Therefore, sample having highest zeta potential was then selected to the following studies. In this time, the amount of CS, 5 and 75 times from initial ratio are selected to test corrosion resistance but 75 times have a high viscosity and difficult to clear.

Figure 4.4 shows the zeta potential values of SiO₂@CS/TPP to confirm CS-crosslinked TPP. In this experiment was varied concentration of TPP (0, 5 and 10 wt%) to study the presence of TPP and effect to corrosion protection. The negative values that obtained indicate TPP (P₃O₁₀⁻⁵) on SiO₂ surface. Therefore, sample that used 5 wt% of concentration is selected to study in next step.

4.3 Surface morphology of coating

In the coating step, particles were mix with GPTMS solution in methanol. Then, drop depositing on the metal substrate before spin coating and dry at 120°C for 12 hrs. The coated sample were characterized using Scanning Electron Microscopy (SEM).

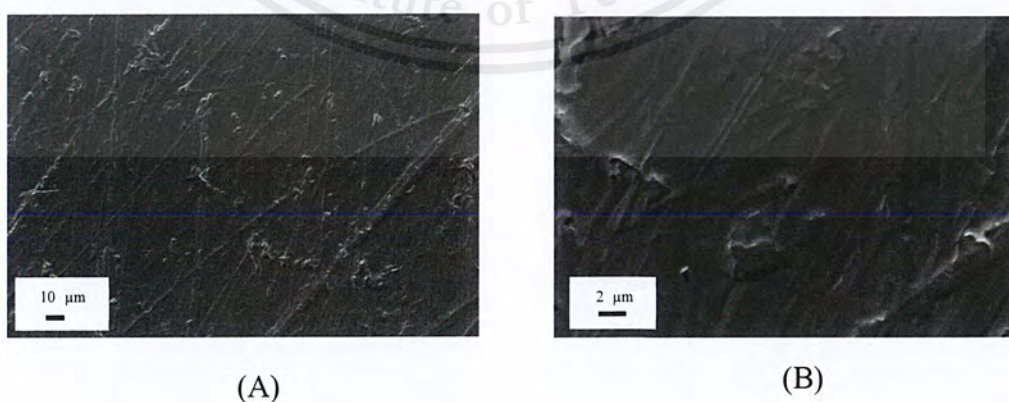


Figure 4.5 SEM image of surface morphology of bare 316L stainless steel (A) magnification 500x, scale bar 10 μm; (B) magnification 3000x, scale bar 2 μm.

This material is reserved for educational use only, not allowed for commercial use.

Forbidden to modify the content, and cite the document when use

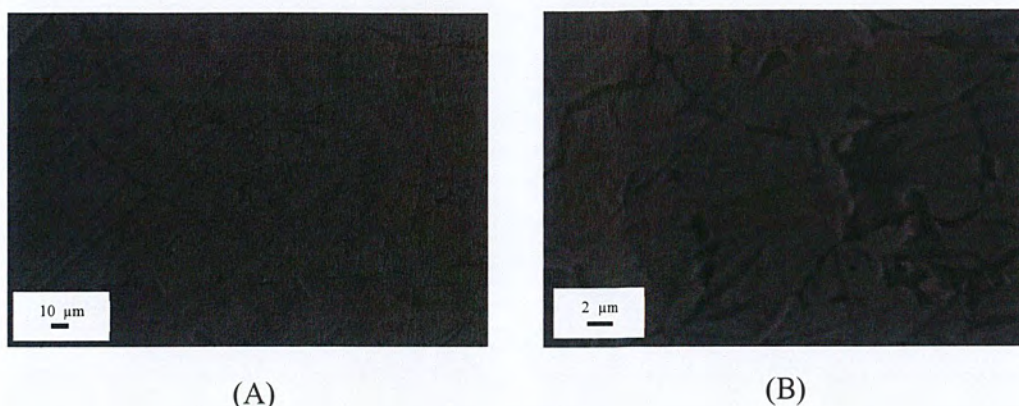


Figure 4.6 SEM image of GPTMS coating or pure epoxy (A) magnification 500x, scale bar 10 μm ; (B) magnification 3000x, scale bar 2 μm .

Figure 4.5 shows surface morphology of bare 316L stainless steel. The surface over the plate present the indents from abrasive paper. Size of indent is less than 2 micrometer. The surface morphology of GPTMS or pure epoxy coating are shown in figure 4.6. The result of their morphology occur the defect on coating. The size of hole is around 4 micrometer might come from the evaporation of water in drying process.

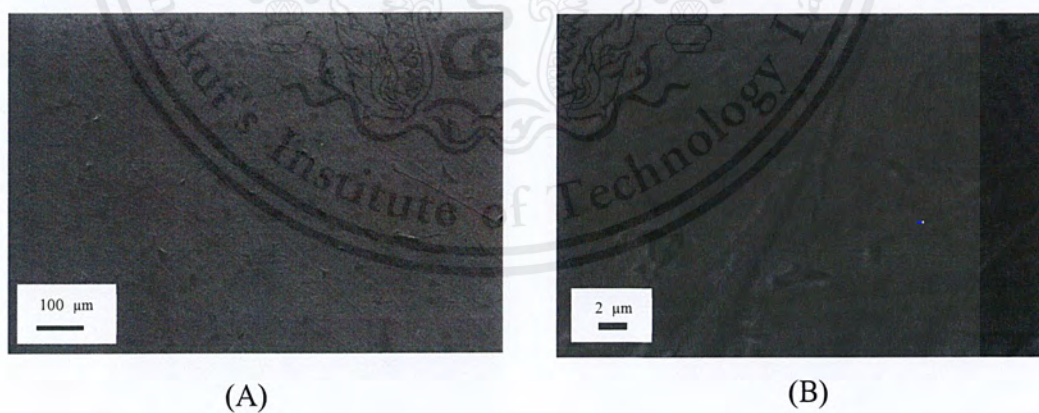


Figure 4.7 SEM image of GPTMS/SiO₂ coating (A) magnification 500x, scale bar 100 μm ; (B) magnification 3000x, scale bar 2 μm .

SEM image of GPTMS/SiO₂ coating are shown in figure 4.7. It was found the smoother surface because addition of SiO₂ nanoparticles act as a filler or pore blocking. These particles have a high thermal expansion efficiency lead to fill the gap from water evaporation and enhanced Young's modulus of the epoxy coating.

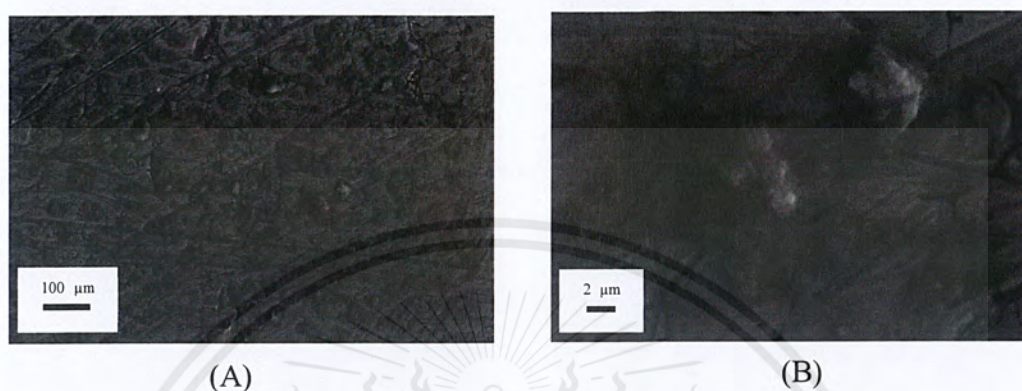


Figure 4.8 SEM image of GPTMS/SiO₂/CS coating (A) magnification 500x, scale bar 100 μm; (B) magnification 3000x, scale bar 2 μm.

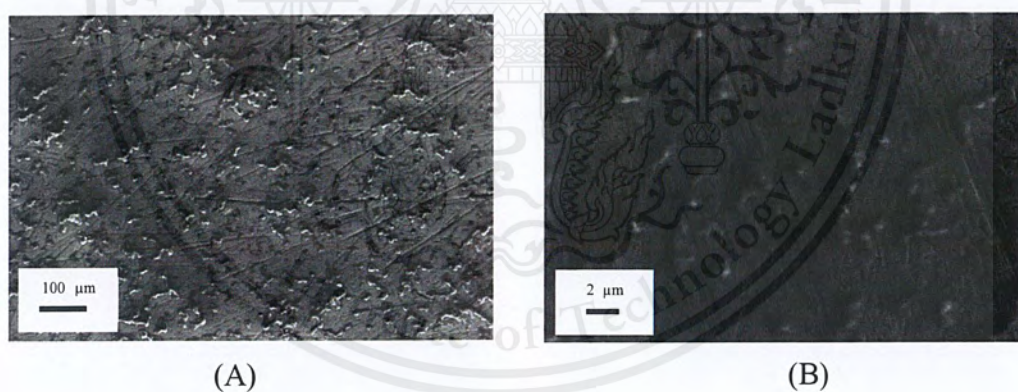


Figure 4.9 SEM image of GPTMS/SiO₂/CS/TPP coating (A) magnification 100x, scale bar 100 μm; (B) magnification 500x, scale bar 2 μm.

Surface morphology of GPTMS/SiO₂/CS and GPTMS/SiO₂/CS/TPP coating are shown in figure 4.8 and 4.9, respectively. In case of GPTMS/SiO₂/CS coating, aggregation of particles were seen through the coating, which supported by zeta potential lower than 30 mV, meaning low colloidal stability. However, GPTMS/SiO₂/CS/TPP coating was used in silica contained epoxy coating result in

occur the greater agglomeration of particles because of crosslinking between CS and TPP result bigger particles, it may be occur the defect on coating.

4.4 Corrosion test

Corrosion resistance of coated steels were tested by using potentiodynamic analysis in 1% NaCl solution which had a pH 6. The resulting, polarization curve of various coating are shown in Figure 4.10 and Figure 4.11

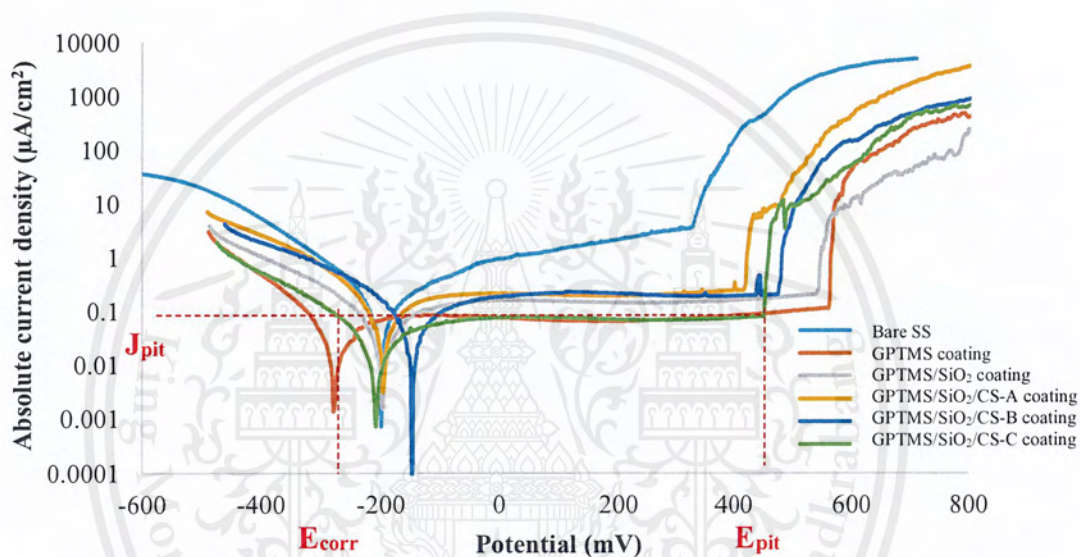


Figure 4.10 Potentiodynamic polarization curves of various coating obtained at potential scan rate of 0.1 mV s^{-1} in 1% NaCl solution at 25°C . Using molecular weight of CS is 25 kDa. A, B, and C denoted concentration of TPP 0, 5, and 10 wt%, respectively.

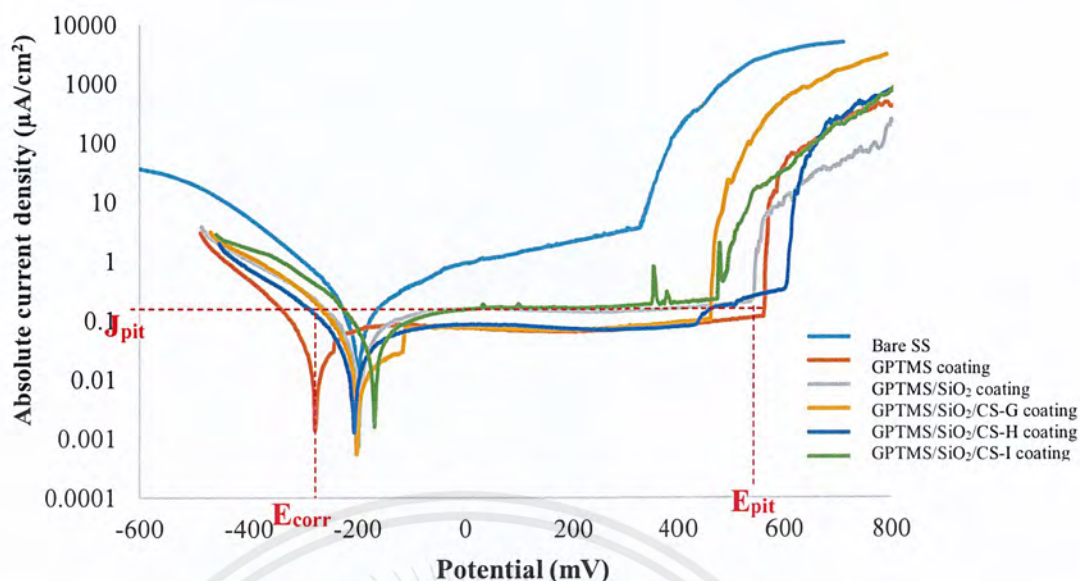


Figure 4.11 Potentiodynamic polarization curves of various coating obtained at potential scan rate of 0.1 mV s^{-1} in 1% NaCl solution at 25°C . Using molecular weight of CS is 890 kDa. G, H, and I denoted concentration of TPP 0, 5, and 10 wt%, respectively.

Polarization curve in Figure 4.10 and 4.11 show the corrosion behavior at various coating. Corrosion potential values (E_{corr}) indicate the coating durability. Corrosion current density (J_{corr}) presents the violence of corrosion rate. Considering the corrosion behavior between bare SS and GPTMS coating, the polarization curve of GPTMS coating show the lower current density in anodic region than bare SS. Silica network between GPTMS molecules acting as a barrier to protect the diffusion of corrosive species results in low corrosion rate, high corrosion resistance²⁴. The GPTMS also increases the passive layer to prevent pitting corrosion. It can be observed from the highest pitting potential value (E_{pit}) which is the potential at the start of pitting corrosion. Although, corrosion potential values (E_{corr}) of GPTMS coating is lower than bare SS, it is more effective corrosion resistance. The lower E_{corr} of GPTMS coating might come from the evaporation of water in drying process²⁵.

Comparing corrosion behavior between GPTMS and GPTMS/SiO₂ coating, pitting potential of GPTMS/SiO₂ give a lower value than GPTMS coating. This result is opposite from the research of Shi et al²⁶. They revealed that silica nanoparticles (15-

20 nm) significantly improved the coating structure and enhanced the corrosion resistance. In our case, it is possible that the difference size (235 ± 34) at the same weight of SiO_2 particles result in decreased the efficiency of pitting corrosion resistance. Therefore, reducing the amount of SiO_2 particles could improve the anticorrosive resistance.

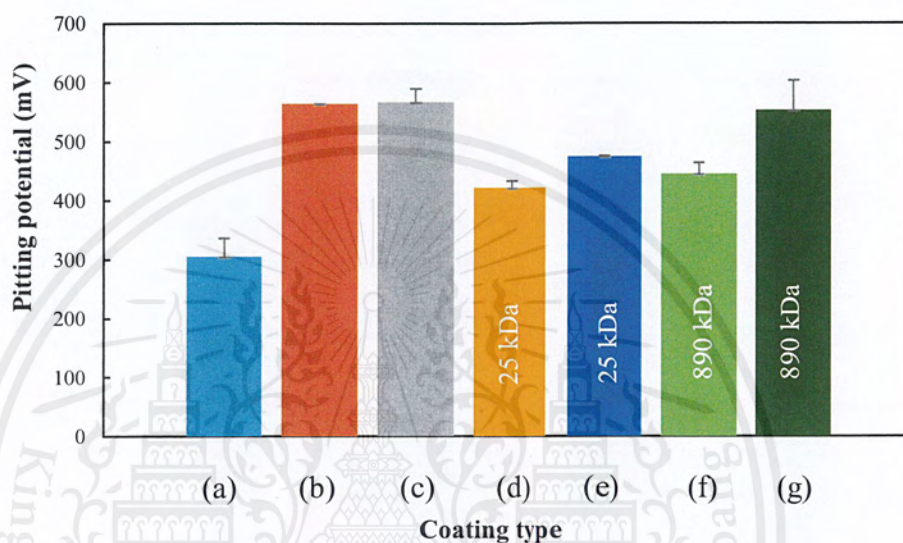


Figure 4.12 Pitting potential value of (a); bare SS (b); GPTMS coating (c); GPTMS/ SiO_2 coating (d-e); GPTMS/ SiO_2 /CS coating (f-g); GPTMS/ SiO_2 /CS/TPP (5 wt%) coating

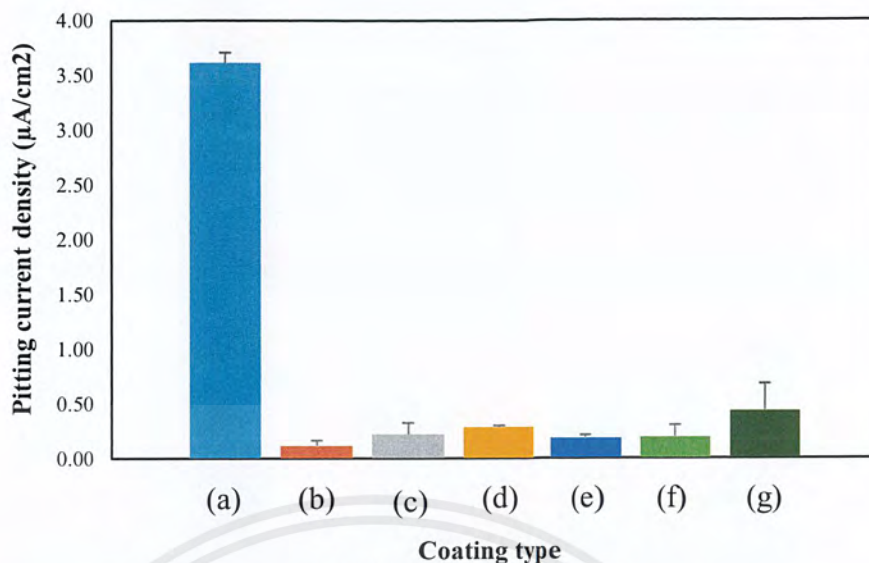


Figure 4.13 Pitting current density value of (a); bare SS (b); GPTMS coating (c); GPTMS/SiO₂ coating (d-e); GPTMS/SiO₂/CS (25 kDa) coating (f-g); GPTMS/SiO₂/CS (890 kDa)/TPP coating

Figure 4.12 and 4.13 show Pitting potential and Pitting current density values of coating, respectively. The pitting corrosion resistance of all GPTMS/SiO₂/CS and GPTMS/SiO₂/CS/TPP coating (D,E,F,G) are lower than pure epoxy coating but they can improve the corrosion protection, decrease the corrosion rate. As a result of these nanocomposite coating are the barrier resistance to enhance the diffusion path length of corrosive species. It is possible that the CS coated on silica coating of D, E, F and G act as the ion trapper from the research of Kartsonakis, et al³. They prepared multilayer coating, one of the layer contain silica particles coated with primary amine groups to trap chloride ion. Next, the GPTMS/SiO₂/CS/TPP coating, there is more efficiency than GPTMS/SiO₂/CS coating because addition of TPP act as the inhibitor result in ion exchange with chloride aion in sodium chloride solution. Followed by the research of Zhou et al⁴. They used layer double hydroxide (LDH) as an anion exchange to trap anion in corrosive enviroment. In addition, all synthesized particle in coatings have efficiency less than GPTMS coating because of aggregation of particles result in defect on coating and lower coating efficiency.

CHAPTER V

CONCLUSION

5.1 Conclusion

Chitosan-coated silica ($\text{SiO}_2@CS$) particles were successfully prepared by using conjugated CS on the SiO_2 surface. Tripolyphosphate was used to crosslink CS shell. Then, the synthesized particles were dispersed in GPTMS solution to coat on metal sheet. The composite coating efficiency were tested using Potentiostat analysis. It was found that the composite coating can use to increase pitting corrosion protection, decrease corrosion rate but low durability. The corrosion resistance of GPTMS coating, GPTMS/ SiO_2 coating, GPTMS/ $\text{SiO}_2@CS/TPP$ coating and GPTMS/ $\text{SiO}_2@CS$ coating tend to decrease due to size and aggregation of particles. The result of corrosion resistance of molecular weight of CS 890 kDa more than 25 kDa. Moreover, the present of TPP on GPTMS/ $\text{SiO}_2@CS/TPP$ coating can improve the corrosion protection, possibly by ion-exchange.

5.2 Suggestions

- 5.2.1. Should study the condition of particles by vary amount of nanoparticles
- 5.2.2. Should study the condition by vary pH of NaCl solution

REFERENCES

- [1] Fontana, M. G.: *Corrosion engineering*; Tata McGraw-Hill Education, 2005.
- [2] Tiwari, A.; Hihara, L.; Rawlins, J.: *Intelligent coatings for corrosion control*; Butterworth-Heinemann, 2014.
- [3] Kartsonakis, I.; Athanasopoulou, E.; Snihirova, D.; Martins, B.; Koklioti, M.; Montemor, M.; Kordas, G.; Charitidis, C. "Multifunctional epoxy coatings combining a mixture of traps and inhibitor loaded nanocontainers for corrosion protection of AA2024-T3". *Corrosion Science* **2014**, *85*, 147-159.
- [4] Zhou, M.; Yan, L.; Ling, H.; Diao, Y.; Pang, X.; Wang, Y.; Gao, K. "Design and fabrication of enhanced corrosion resistance Zn-Al layered double hydroxides films based anion-exchange mechanism on magnesium alloys". *Applied Surface Science* **2017**, *404*, 246-253.
- [5] Qian, B.; Song, Z.; Hao, L.; Fan, H. "Entrapment of polyaspartic acid on silica nanoparticle for self-healing coatings". *Materials and Corrosion* **2017**.
- [6] Gierszewska, M.; Ostrowska-Czubenko, J. "Chitosan-based membranes with different ionic crosslinking density for pharmaceutical and industrial applications". *Carbohydrate polymers* **2016**, *153*, 501-511.
- [7] Khatak, H. S.; Raj, B.: *Corrosion of austenitic stainless steels: mechanism, mitigation and monitoring*; Elsevier, 2002.
- [8] Clum, J. A. Ferrous Production Metallurgy. *JOM* **1982**, *34*, 54-54.
- [9] Speller, F. N.: *Corrosion Causes and Prevention: An Engineering Problem*; McGraw-Hill Book Company, Inc.; New York, 1926.
- [10] Frankel, G. "Pitting corrosion of metals a review of the critical factors". *Journal of the Electrochemical Society* **1998**, *145*, 2186-2198.
- [11] Saji, V. S.; Cook, R.: *Corrosion protection and control using nanomaterials*; Elsevier, 2012.
- [12] Shi, X.; Nguyen, T. A.; Suo, Z.; Liu, Y.; Avci, R. Effect of nanoparticles on the anticorrosion and mechanical properties of epoxy coating. *Surface and Coatings Technology* **2009**, *204*, 237-245.
- [13] Kongparakul, S.; Kornprasert, S.; Suriya, P.; Le, D.; Samart, C.; Chantarasiri, N.; Prasassarakich, P.; Guan, G. "Self-healing hybrid nanocomposite anticorrosive coating from epoxy/modified nanosilica/perfluorooctyl triethoxysilane". *Progress in Organic Coatings* **2017**, *104*, 173-179.
- [14] Kartsonakis, I.; Balaskas, A.; Koumoulos, E.; Charitidis, C.; Kordas, G. "Evaluation of corrosion resistance of magnesium alloy ZK10 coated with hybrid organic-inorganic film including containers". *Corrosion science* **2012**, *65*, 481-493.
- [15] Callister, W. D.; Rethwisch, D. G.: *Materials science and engineering*; John Wiley & Sons NY, 2011; Vol. 5.
- [16] Tedim, J.; Kuznetsova, A.; Salak, A.; Montemor, F.; Snihirova, D.; Pilz, M.; Zheludkevich, M.; Ferreira, "M. Zn-Al layered double hydroxides as chloride nanotraps in active protective coatings". *corrosion Science* **2012**, *55*, 1-4.
- [17] Ramezanzadeh, B.; Niroumandrad, S.; Ahmadi, A.; Mahdavian, M.; Moghadam, M. M. "Enhancement of barrier and corrosion protection performance of an epoxy coating through wet transfer of amino functionalized graphene oxide". *Corrosion Science* **2016**, *103*, 283-304.
- [18] Luckachan, G. "Self-healing Anticorrosion Coatings for Gas Pipelines and Storage Tanks". *Corrosion Science and Technology* **2016**, *15*, 209-216.

- [19] Morocco, C. "Sodium tripolyphosphate (STPP) as a novel corrosion inhibitor for mild steel in 1 M HCl". *Journal of optoelectronics and advanced materials* **2013**, *15*, 451-456.
- [20] Huang, Y.; Pemberton, J. E. "Synthesis of uniform, spherical sub-100 nm silica particles using a conceptual modification of the classic LaMer model". *Colloids and Surfaces A: Physicochemical and engineering aspects* **2010**, *360*, 175-183.
- [21] Zhou, L.; Jia, Y.; Peng, J.; Liu, Z.; Al-Zaini, E. "Competitive adsorption of uranium(VI) and thorium(IV) ions from aqueous solution using triphosphate-crosslinked magnetic chitosan resins". *Journal of Radioanalytical and Nuclear Chemistry* **2014**, *302*, 331-340.
- [22] Deng, Z.; Zhen, Z.; Hu, X.; Wu, S.; Xu, Z.; Chu, P. K. "Hollow chitosan-silica nanospheres as pH-sensitive targeted delivery carriers in breast cancer therapy". *Biomaterials* **2011**, *32*, 4976-4986.
- [23] Gan, Q.; Wang, T.; Cochrane, C.; McCarron, P. "Modulation of surface charge, particle size and morphological properties of chitosan-TPP nanoparticles intended for gene delivery". *Colloids and Surfaces B: Biointerfaces* **2005**, *44*, 65-73.
- [24] Yuan, X.; Yue, Z.; Chen, X.; Wen, S.; Li, L.; Feng, T. "The protective and adhesion properties of silicone-epoxy hybrid coatings on 2024 Al-alloy with a silane film as pretreatment". *Corrosion Science* **2016**, *104*, 84-97.
- [25] Metroke, T. L.; Parkhill, R. L.; Knobbe, E. T. "Passivation of metal alloys using sol-gel-derived materials—a review". *Progress in Organic Coatings* **2001**, *41*, 233-238.
- [26] Palraj, S.; Selvaraj, M.; Maruthan, K.; Rajagopal, G. "Corrosion and wear resistance behavior of nano-silica epoxy composite coatings". *Progress in Organic Coatings* **2015**, *81*, 132-139.



This material is reserved for educational use only, not allowed for commercial use.

Forbidden to modify the content, and cite the document when use

APPENDIX A

EXPERIMENTAL DATA

A.1 Synthesis of silica nanoparticles

Table A.1 Chemical composition ratio in silica nanoparticles synthesis

SiO ₂	Tetraethyl orthosilicate	Ammonium hydroxide	Deionized water	Methanol
Ratio	1	2.5	2	20

A.2 Analytical measurements

Table A.2 List of analytical measurement that use study characterization

Analytical measurement	Abbreviation	Detail
Transmission electron microscope	TEM	FEI TECNAI T20 G2
Fourier transform infrared spectroscopy	FTIR	Perkin Elmer, Spectra GX
Potentiostat	-	Autolab PGSTAT302N
Zetasizer	-	Nano ZS, Malvern measurement
Scanning Electron Microscopy	SEM	EVO MA 10 Versatile multipurpose SEM

APPENDIX B

RESULTS DATA

B.1 Zeta potential data of SiO₂ nanoparticles

Table B.1 Zeta potential value of SiO₂ nanoparticles

Sample	Zeta potential (mV)
SiO ₂	-45.8

B.2 Zeta potential data by varying amount of CS (times from initial ratio)

Table B.2 Zeta potential values of SiO₂@CS particles varying amount of CS

Ratio of coating material composition		Zeta potential (mV)
MW of chitosan	Amount of chitosan (times)	
25 kDa	5	10.83
	25	8.25
	50	9.18
	75	13.53
	100	5.37
890 kDa	5	9.78
	25	3.03
	50	12.87
	75	20.43
	100	12.07

B.3 Zeta potential data by varying concentration of TPP (wt%)

Table B.3 Zeta potential values of SiO₂@CS/TPP particles varying concentration of TPP

Coating material composition		Zeta potential (mV)
MW of chitosan	Concentration of TPP (wt%)	
25 kDa	5	-9.41
	10	-7.66
890 kDa	5	-10.39
	10	-10.70

B.4 Pitting potential and Pitting current density of sample

Table B.4 Pitting potential and pitting current density of bare SS and various coating

Coating	Pitting potential (mV)	Pitting current density ($\mu\text{A}/\text{cm}^2$)
Bare SS	328.15	3.73
GPTMS coating	560.09	0.11
GPTMS/SiO ₂ coating	529.23	0.22
GPTMS/SiO ₂ /CS (25 kDa) coating	421.93	0.28
GPTMS/SiO ₂ /CS (890 kDa) coating	474.24	0.18
GPTMS/SiO ₂ /CS (25 kDa)/TPP coating	444.45	0.19
GPTMS/SiO ₂ /CS (890 kDa)/TPP coating	552.14	0.43

B.5 Efficiency of pitting corrosion protection (%)

Table B.5 Efficiency of pitting corrosion protection (%) of bare SS and various coating

Coating	Efficiency of pitting corrosion protection (%)	
	Comparison of pitting current density	Comparison of pitting potential
Bare SS	ref.	-
GPTMS coating	96.95	ref.
GPTMS/SiO ₂ coating	93.88	00.49
GPTMS/SiO ₂ /CS-A coating	92.22	25.23
GPTMS/SiO ₂ /CS-B coating	95.04	15.83
GPTMS/SiO ₂ /CS-C coating	97.50	12.97
GPTMS/SiO ₂ /CS-G coating	97.46	21.12
GPTMS/SiO ₂ /CS-H coating	88.17	02.00
GPTMS/SiO ₂ /CS-I coating	95.60	13.03

B.6 FTIR spectra of SiO₂@CS at various CS concentration (25 KDa)

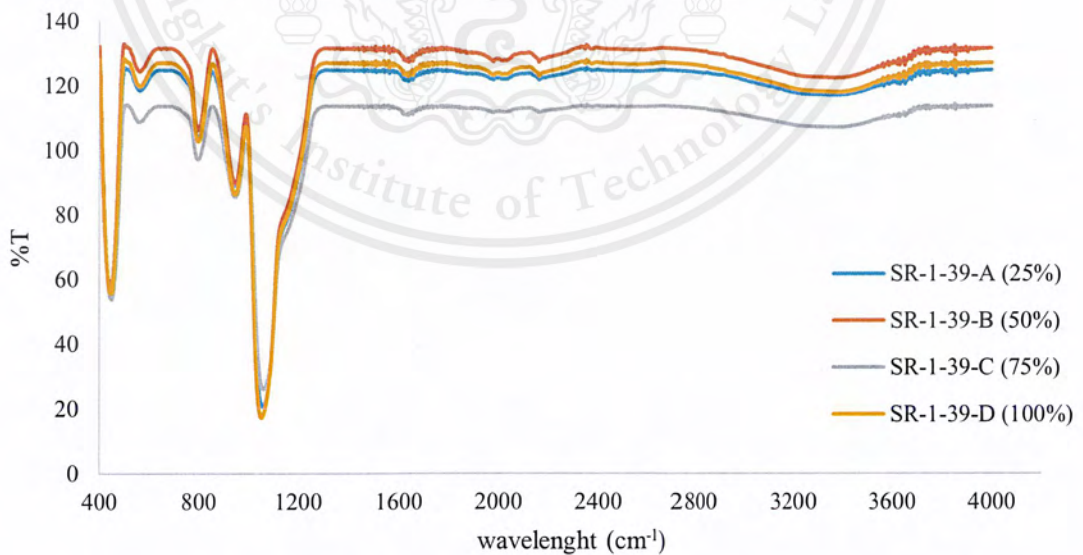
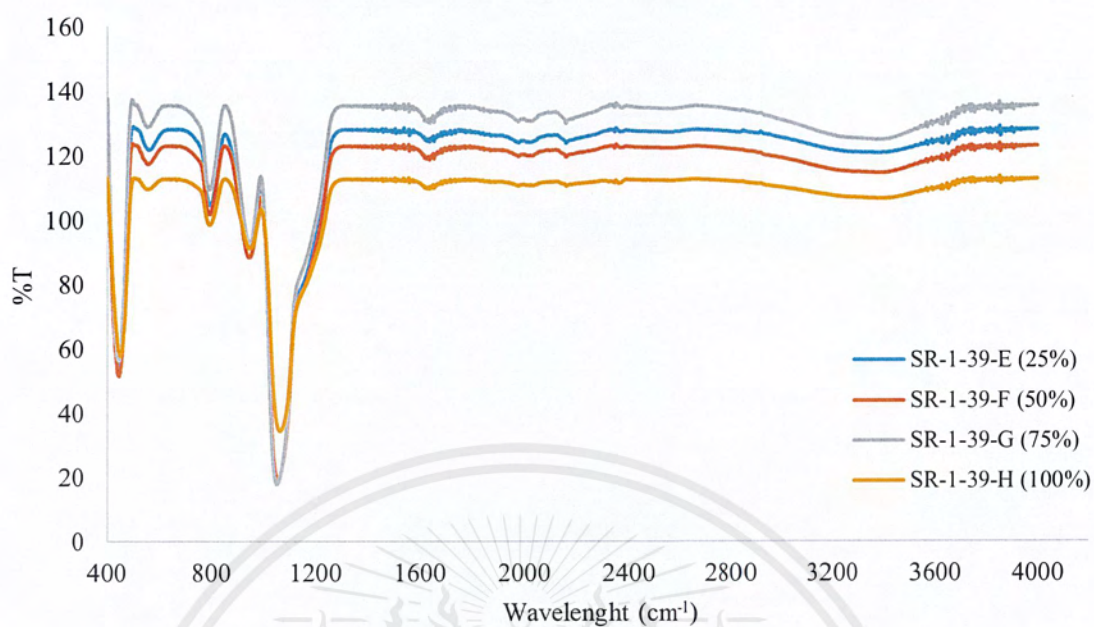


Figure B.6 spectra of SiO₂@CS at various CS concentration (25 KDa)

B.7 FTIR spectra of SiO₂@CS at various CS concentration (890 KDa)**Figure B.7** spectra of SiO₂@CS at various CS concentration (890 KDa)

APPENDIX C

CALCULATION DATA

C.1 Calculate the effectiveness of pitting corrosion protection.

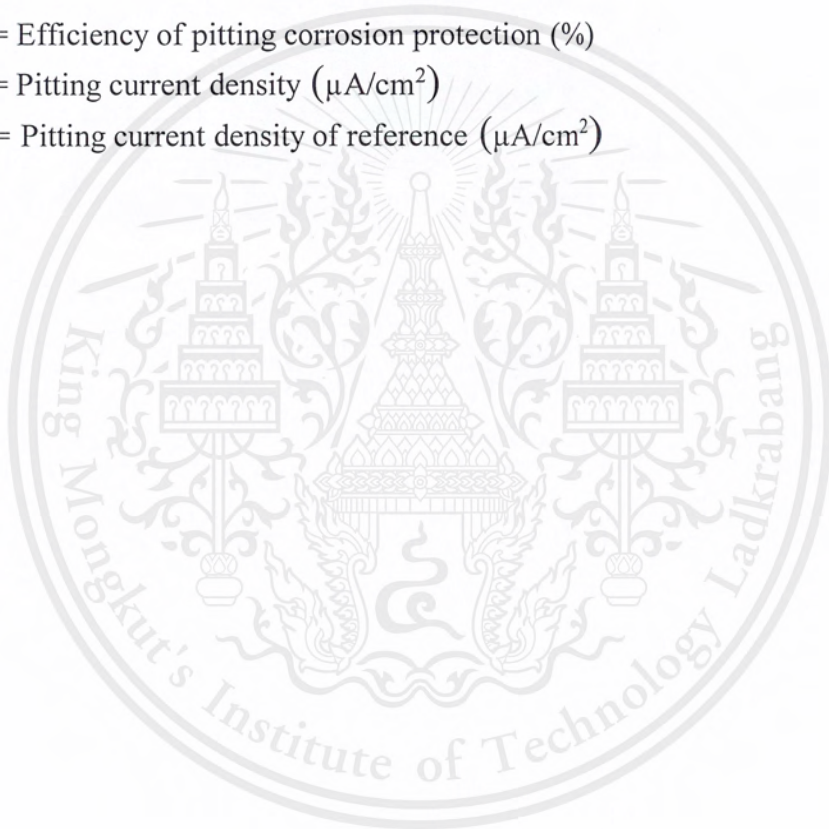
Efficiency of pitting corrosion protection can be calculated from the below equation.

$$\eta_{pit} = \frac{|J_{pit} - J_{pit,ref}|}{J_{pit,ref}} \times 100$$

η_{pit} = Efficiency of pitting corrosion protection (%)

J_{pit} = Pitting current density ($\mu\text{A}/\text{cm}^2$)

$J_{pit,ref}$ = Pitting current density of reference ($\mu\text{A}/\text{cm}^2$)



BIOGRAHPY

Name: Sasiprapa Rattananukul
Date of Birth: 17/07/1995
Address: 154/101 Moo10 Nongprue, Banglamung, Chonburi 20150
E-mail: s.rattananukul@gmail.com

Academic Background:

2011-2013 Singsamut school
2014-2017 King Mongkut's Institute of Technology Ladkrabang,
Petrochemical Engineering

Working Experience: Internship at PTT global chemical Co. Ltd.

